J. Fluid Mech. (1975), *vol.* 69, *part* 1, *pp.* 73–95
Printed in Great Britain

Experiments on the instability waves in a supersonic jet and their acoustic radiation

By DENNIS K. McLAUGHLIN, GERALD L. MORRISON AND TIMOTHY R. TROUTT
Oklahoma State University, Stillwater, Oklahoma

(Received 21 January 1974)

An experimental investigation of the instability and the acoustic radiation of the low Reynolds number axisymmetric supersonic jet has been performed. Hot-wire measurements in the flow field and microphone measurements in the acoustic field were obtained from different size jets at Mach numbers of about 2. The Reynolds number ranged from 8000 to 107 000, which contrasts with a Reynolds number of $1{\cdot}3 \times 10^6$ for similar jets exhausting into atmospheric pressure.

Hot-wire measurements indicate that the instability process in the perfectly expanded jet consists of numerous discrete frequency modes around a Strouhal number of 0·18. The waves grow almost exponentially and propagate downstream at a supersonic velocity with respect to the surrounding air. Measurements of the wavelength and wave speed of the $St = 0{\cdot}18$ oscillation agree closely with Tam's theoretical predictions.

Microphone measurements have shown that the wavelength, wave orientation and frequency of the acoustic radiation generated by the dominant instability agree with the Mach wave concept. The sound pressure levels measured in the low Reynolds number jet extrapolate to values approaching the noise levels measured by other experimenters in high Reynolds number jets. These measurements provide more evidence that the dominant noise generation mechanism in high Reynolds number jets is the large-scale instability.

1. Introduction

The major obstacle to a complete theory in jet noise analysis has been the identification of the fluctuations in the jet which generate the radiated sound. Lighthill's classical formulation (1952, 1954) provided the groundwork for relating the acoustic radiation to the disturbances in the jet; and his basic theory, first applied to subsonic jets, has been extended by several authors into the supersonic regime. (See e.g. Ffowcs Williams 1963; Ribner 1969.) However, in these analyses, information about the flow disturbances formulated in terms of the Lighthill stress tensor T_{ij} has not come from the fundamental laws of fluid dynamics, but from turbulence models based on empirical evidence.

Recently, a number of investigators have attempted to formulate the flow disturbances in terms of instability waves governed, at least to some extent, by variations in the classical laminar hydrodynamic stability theory. Crow &

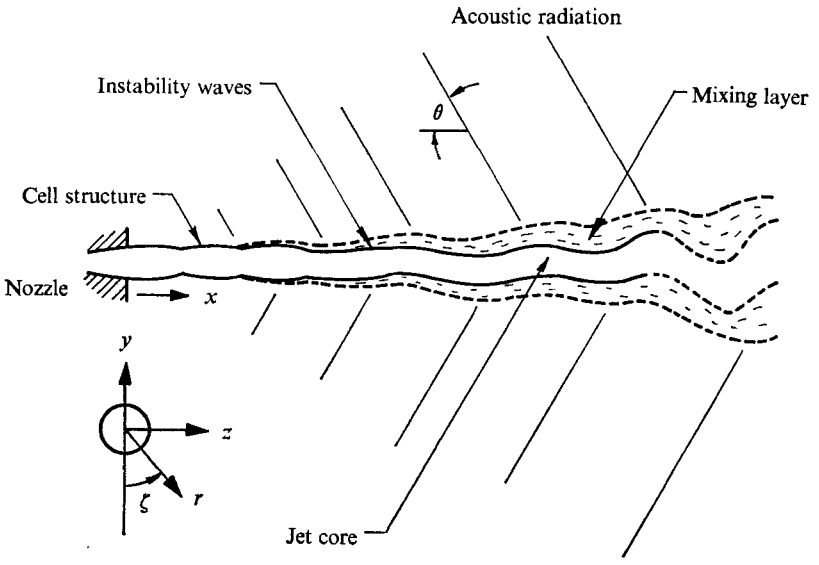

FIGURE 1. General features of the supersonic jet and its acoustic radiation.

Champagne (1971) have demonstrated that there is an orderly structure in the subsonic jet, whose characterization can be undertaken with the help of the instability properties of the jet. Lilley *et al.* (1973) have reported some progress in using this concept in further development of noise prediction of the subsonic jet.

In the area of supersonic jet noise analysis several authors (e.g. Tam 1971, 1972, 1973; Sedel'nikov 1967; Chan & Westley 1973) have used stability theory to describe the disturbances within the jet. At this time Tam has progressed the furthest toward producing a useful and complete analysis. Although there are many similarities between the subsonic and supersonic jet noise phenomena, there are differences in the generation mechanisms which tend to be of a fundamental nature. First of all, in any supersonic jet there exists a cell structure of expansion and compression waves. Even though these may be of infinitesimal strength, there is substantial evidence that they can have a controlling influence on the behaviour of the disturbances within the jet. Second, the acoustic radiation emitted from the supersonic part of the jet has a definite degree of order to it, not present in the subsonic jet. Figure 1 is a schematic, showing some of these features of the supersonic jet. The orderly behaviour of some of the flow and acoustic properties suggests that increased understanding may result from an analysis which capitalizes on these deterministic phenomena.

The fundamental idea of Tam's theory (supported in this by Bishop, Ffowcs Williams & Smith 1971, and others) is that the dominant noise producing mechanism is a large-scale undulation of the full jet flow. This undulation closely resembles the initial laminar instability with small-scale random turbulence superimposed upon it. Although Tam's theory contains a large number of simplifying assumptions, it has been surprisingly accurate in predicting many of the acoustic radiation properties of the supersonic jet.

One of the particularly encouraging features of the theory is that it is derived from the fundamental laws of fluid dynamics, albeit greatly simplified, and the only empirical evidence used is information about the mean flow properties.

There is considerable experimental evidence on the nature of the flow disturbances in the case of the subsonic jet (see, e.g., Crow & Champagne 1971; Lee & Ribner 1972). For the supersonic jet, however, there is a dearth of definitive measurements of the flow disturbances and their relationship to the acoustic radiation.

The goal of our research programme is to provide the flow and acoustic measurements necessary to stimulate a complete development of the instability approach to the supersonic jet noise problem. There are many critical aspects that must be tested before a reasonable judgement on its applicability can be made. Thus, the major objectives of the research are to answer the following questions. (i) Do the flow disturbances propagate and grow in a way consistent with stability analysis? (ii) Are the acoustic radiation properties consistent with generating disturbances that can be modelled as instability waves? These are general questions, that must be answered by experiments studying the details of the flow and noise processes.

To accomplish the goal of providing the experimental foundation for the instability analysis, we have taken the approach of first testing the theory under its most favourable conditions. Being a linear theory, it should predict the *initial* instabilities in the transition process from laminar to turbulent flow. To test this, it is necessary to run the jet at a Reynolds number low enough to yield initially laminar flow. We obtain the low Reynolds numbers by exhausting the jet into a chamber whose pressure is maintained at about $\frac{1}{30}$ of an atmosphere. At Reynolds numbers around 15 000 (at $M = 2{\cdot}3$), the jet is laminar for several diameters; and the initial fluctuations measured in the flow are the instabilities of the laminar flow (see McLaughlin & McColgan 1974). The Reynolds number of 15 000 contrasts with the value $1{\cdot}3 \times 10^6$ one obtains with an $M = 2{\cdot}3$, 10 mm diameter jet exhausting to atmosphere. It is important to recognize that the instabilities in the laminar flow will probably not be quantitatively the same as the large-scale instabilities in the turbulent jet. However, it may be reasonable to assume that their qualitative behaviour, and their influence on the acoustic radiation, will be similar.

To determine what specific measurements must be made in this stability investigation, consider the elementary wave representation of any fluctuating quantity

$$q(x, r, \zeta, t) = \hat{q}(r) \exp\left[i(kx - \omega t - n\zeta)\right].$$

A complete stability investigation includes the measurement of the interdependence of the eigenvalues k and ω corresponding to each azimuthal mode number n and the eigenfunction $\hat{q}(r)$ for each n, k, ω combination. Since the stability theories of Tam (1972) and Sedel'nikov (1967) have been evaluated in terms of spatially growing waves, we shall follow the same approach in this study. Hence, $k = k_R + ik_I$ and ω is taken to be pure real. In this formulation k_R is the wavenumber in the x direction, $-k_I$ is the spatial amplification rate for exponential growth, and ω is the frequency of the fluctuation.

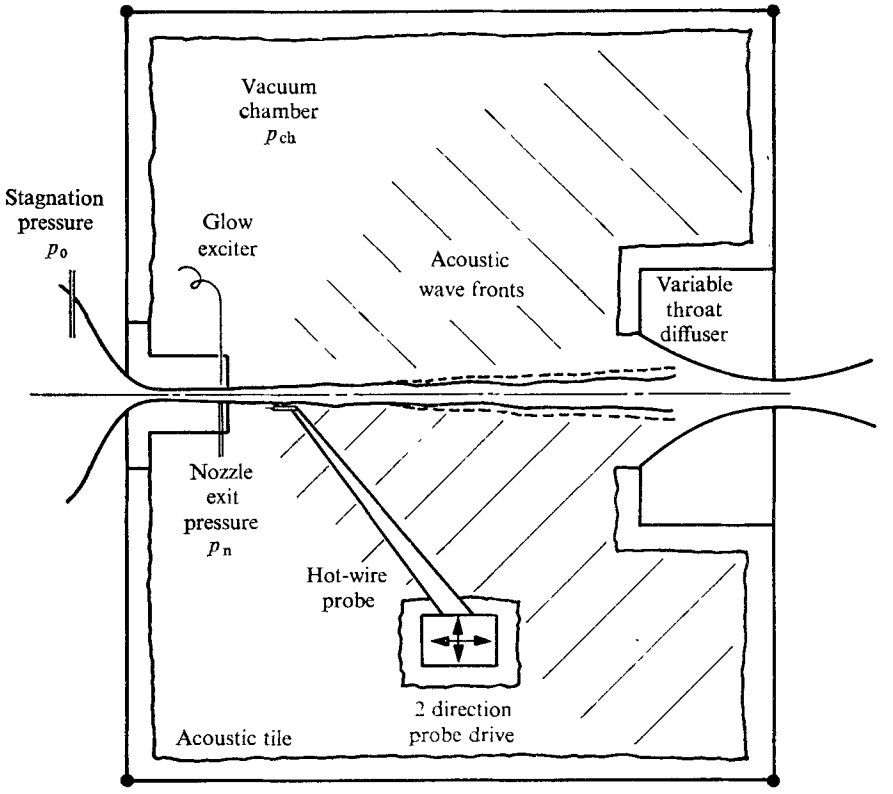

FIGURE 2. Schematic of the supersonic jet test facility.

Since one of our major objectives is to investigate whether or not the acoustic radiation properties are consistent with generating disturbances that can be modelled as instability waves, it is particularly important to measure those dispersion properties that can be compared directly with the acoustic waves. The most obvious comparison is in the frequencies of the dominant oscillations. In addition, the present investigation relies on a comparison of wavelengths in the x direction of both the instability and acoustic waves. Similarity in the basic wave structures is important in demonstrating the cause and effect relationship between the flow instabilities and the radiated noise.

2. Description of the experiment

A schematic of the basic facility is shown in figure 2. One of three different sized axisymmetric supersonic de Laval nozzles of area ratio 3·036 was located on the inside wall of a vacuum chamber, whose pressure p_{ch} was controlled by a variable area exit diffuser. The inlet to the jet was a 15 cm diameter stilling section, whose cross-sectional area was at least 150 times greater than the jet exit area. In the stilling section, behind the control valve, was a 5 cm section of foam rubber and six fine screens.

The vacuum chamber was isolated from pump vibrations by a 30 m^3 vacuum storage tank and 15 m of piping. To reduce the reverberant sound pressure field, the vacuum chamber was lined with 1·5 cm acoustic tile.

The three nozzles had exit diameters D of 6·35, 9·52 and 15·9 mm; but the majority of the measurements were made with the two smaller nozzles. Since the nozzles all have the same area ratio, the exit Mach numbers differed slightly owing to viscous effects. The three nozzles were used to show that the phenomena measured are characteristic of the jet flow and not the flow facility. The 6·35 and 9·52 mm nozzles had simple conical contours, with half-angles of 1·60 and 2·28°, respectively. The 15·9 mm nozzle had contoured walls designed by the method of characteristics to provide uniform flow at the nozzle exit. The total Reynolds number envelope includes measurements from $Re = 8\,000$ to 107 000. The stagnation temperature T_0 for all measurements is atmospheric temperature (530 °R).

To determine the actual jet Mach number and other mean flow properties accurately, Pitot and static pressure measurements were made in the jet flow fields. The Pitot probe used was a standard square-ended probe, approximately 0·2 mm in outside diameter, of the type calibrated by Matthews (1958). The static pressure probe was a slender (1 mm diameter) cone cylinder, identical in shape to the probe extensively calibrated by Behrens (1963). If the stagnation temperature in the jet is assumed constant, then the two pressure measurements are all that is needed for a complete determination of the local mean flow properties. The assumption of constant T_0 is probably valid along the centre-line, but not in the shear annulus of the jet.

Flow-field fluctuation measurements were made with a Disa Model 55D01 constant-temperature hot-wire anemometer set. The probes consisted of Disa Model 55A53 sub-miniature probes epoxied to the upper edge of slender brass wedges (shown in figure 2). Acoustic measurements were made with a $\frac{1}{8}$ in. diameter Bruel & Kjaer condenser microphone type 4138. This microphone had omni-directional response within $\pm$ 3 dB for frequencies up to 60 kHz. In the case of both the hot-wire and microphone instrumentation, the manufacturer's specified frequency response exceeded 50 kHz. This far exceeds the frequency range of measurements presented here.

A two degree of freedom probe drive was located inside the vacuum chamber to support any of the pressure, hot-wire or microphone probes. The drive was capable of moving the probe axially and vertically throughout the centre-line plane of the jet. A ten turn precision potentiometer provided a d.c. voltage proportional to the vertical probe position used in generating continuous hot-wire mean or fluctuating voltage profiles on a Moseley Model 2D XY Recorder. Spectral analysis output data was also plotted on the XY recorder. The present spectra were taken with a Hewlett Packard Model 302 A wave analyser, with a bandwidth of 6 Hz. A General Radio Model 1910 A wave analyser, with a bandwidth of 100 Hz, was used to check the results obtained with the narrow-band analyser.

Wave-front orientations and wavelengths of a spectral component of flow fluctuations in the jet and acoustic fluctuations outside the jet were obtained from relative phase measurements. The phase measurements were made by a glow

discharge excitation technique, similar to that used by Kendall (1967). The phase of the spectral component of the hot-wire or microphone signal was compared with the signal input to the modulating glow discharge. The glow was set up at a single point tungsten electrode, approximately 2 mm from the jet exit. The simple electronic circuit used consisted of an a.c. voltage of 800 V peak to peak, biased to a negative potential by a 450 V d.c. supply, which drew about 2 m amp.

3. Experimental results

3.1. *Mean flow measurements*

Pitot pressure and static pressure probe measurements were made on the centre-line of the two smaller jets in the near vicinity of the exit. Local jet Mach numbers were evaluated from these measurements, and showed some degree of wave-cell structure, as depicted schematically in figure 1, even when the jet was perfectly expanded (ratio of nozzle exit pressure p_n to jet back pressure p_{ch} was held at between 1·00 and 1·01). The average Mach numbers (on the centre-line, between the exit and two diameters downstream) were $M = 2{\cdot}2$ (6·35 mm jet) and 2·3 (9·52 mm jet). The Mach number in this region of the 15·9 mm jet was estimated from hot-wire measurements to be 2·5.

Complete and accurate hot-wire anemometer measurements in low-density high-speed flows require a lengthy data reduction scheme, primarily because of the great amount of heat conduction down the wire to the supports (see e.g. Dewey 1965). To accomplish the objectives outlined in §1, it was not necessary to know the exact amplitude of the hot-wire voltage fluctuations, or to know how they decomposed into velocity, temperature and pressure fluctuations (as explained by Morkovin 1956). However, some measurements were made using Morkovin's modal decomposition technique, which demonstrated that the stagnation temperature fluctuations were much smaller than the mass flux fluctuations, and contributed little to the hot-wire signal. For this reason, the hot-wire voltage data will be presented on arbitrary linear scales, and following Behrens (1968), interpreted to be roughly proportional to mass flux (ρu).

Centre-line measurements of mean hot-wire voltage were made in the two smaller jets to demonstrate the effect of pressure balance condition (p_n/p_{ch}) on the mean flow cell structure. The measurements in the 6·35 mm jet are depicted in figures 3 (*a*) and (*b*), for two values of the pressure balance condition. Notice that, even in the perfectly-expanded jet, there is a degree of wave-cell structure, although it is naturally much weaker than in the under-expanded jet. In the perfectly-expanded 6·35 mm jet, the excursions in mass flux are $\pm 6\,\%$ of the mean value, and excursions in Mach number are $\pm 3{\cdot}5\,\%$ of $M = 2{\cdot}2$. The absolute magnitudes of these estimates are obtained from the limited measurements made with the Pitot and static pressure probes, which are assumed to be more accurate than estimates based on a rough hot-wire calibration.

Figure 3 (*c*) is the result of hot-wire measurements in the perfectly-expanded 9·52 mm jet, at the same unit Reynolds number, and with the same hot-wire probe and overheat ratio, as was used in the small-nozzle measurements (figures 3 (*a*), (*b*)). This comparison shows that the wave-cell structure is at least twice as

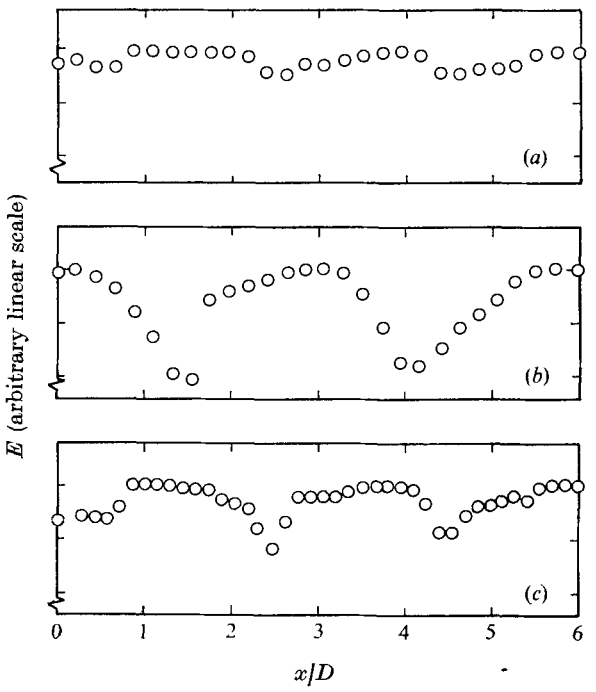

FIGURE 3. Axial distribution of centre-line mean hot-wire voltage E, showing flow variations.

	D (mm)	p_n/p_{ch}	Re
(*a*)	6·35	1·01	14 500
(*b*)	6·35	1·5	14 400
(*c*)	9·52	1·01	20 000

strong in the perfectly-expanded 9·52 mm jet compared with the 6·35 mm jet. This was no doubt because of the larger divergence angle of the larger nozzle. We believe the result has important consequences in the instability process, as will be pointed out below.

Figure 4 is included to give the reader an idea of the mean flow profile of the two smaller jets for two representative Reynolds numbers. (Recall that mean mass flux is approximately proportional to mean hot-wire bridge voltage.) This figure indicates that the profiles can be approximated with a top-hat shape (sometimes called plug flow) to a reasonable degree of accuracy for at least 4 diameters of the jet flow. The top-hat profile is used for most theoretical stability analyses (Tam 1971, 1972; Sedel'nikov 1967; Chan & Westley 1973). The measurements of figure 4 were made in the perfectly-expanded jet ($p_n/p_{ch} \simeq 1{\cdot}01$), as were the rest of the measurements presented here.

3.2. *Microphone and hot-wire spectra*

Figure 5 presents representative microphone spectra measured in the acoustic field of the three supersonic jets. The probe was located approximately 8 diameters downstream of the exit, and 4 diameters below the jet centre-line. The

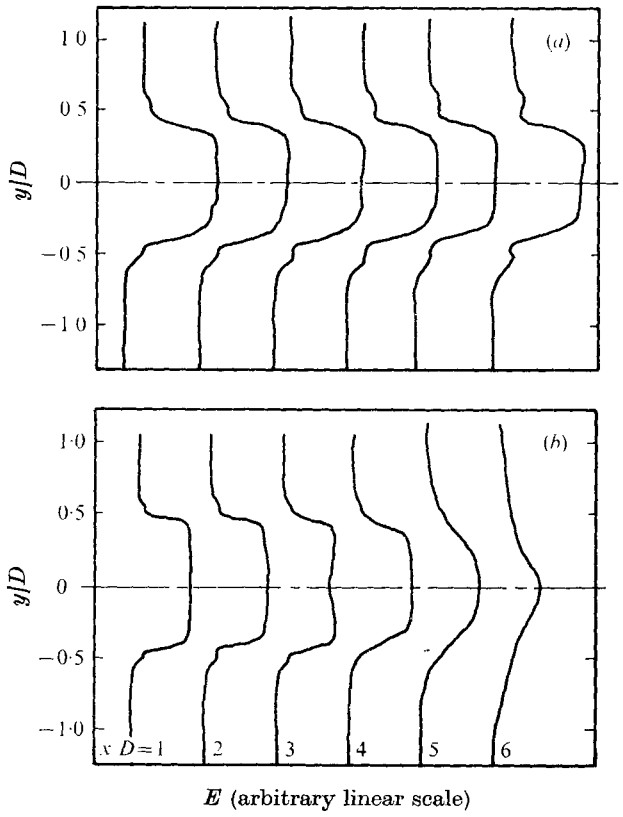

FIGURE 4. Profiles of mean hot-wire voltage E, at various downstream locations.

	D (mm)	p_n/p_{ch}	Re
(a)	6·35	1·01	14 700
(b)	9·52	1·02	47 100

data are presented in terms of the non-dimensional frequency $St = fd/U$, where U is the mean centre-line jet velocity, and d is the effective jet diameter (the exit diameter of the nozzle D, minus twice the displacement thickness of the boundary layer at the nozzle exit). The reason for presenting data from jets of three sizes is to demonstrate that the dominant spectral components, being at similar Strouhal numbers, are phenomena characteristic of the jet, not the flow facility. Notice however, that in all three spectra there is a large low-frequency content at $St = 0{\cdot}02$ or less. This low-frequency noise was mostly due to vacuum chamber resonance, and is therefore filtered out of most amplitude measurements presented below.

The universal character of the spectra shown in figure 5 is strong evidence that the dominant mode behaviour of the jet is not an acoustic feed-back from either a probe or some part of the vacuum chamber. But additional acoustic qualification experiments were performed on the test chamber, to prove its adequacy for these measurements. From reverberation time measurements it was established that the reverberant pressure field contributes less than 3 dB to the measured sound pressure field. Other noise contributions from background sources (such

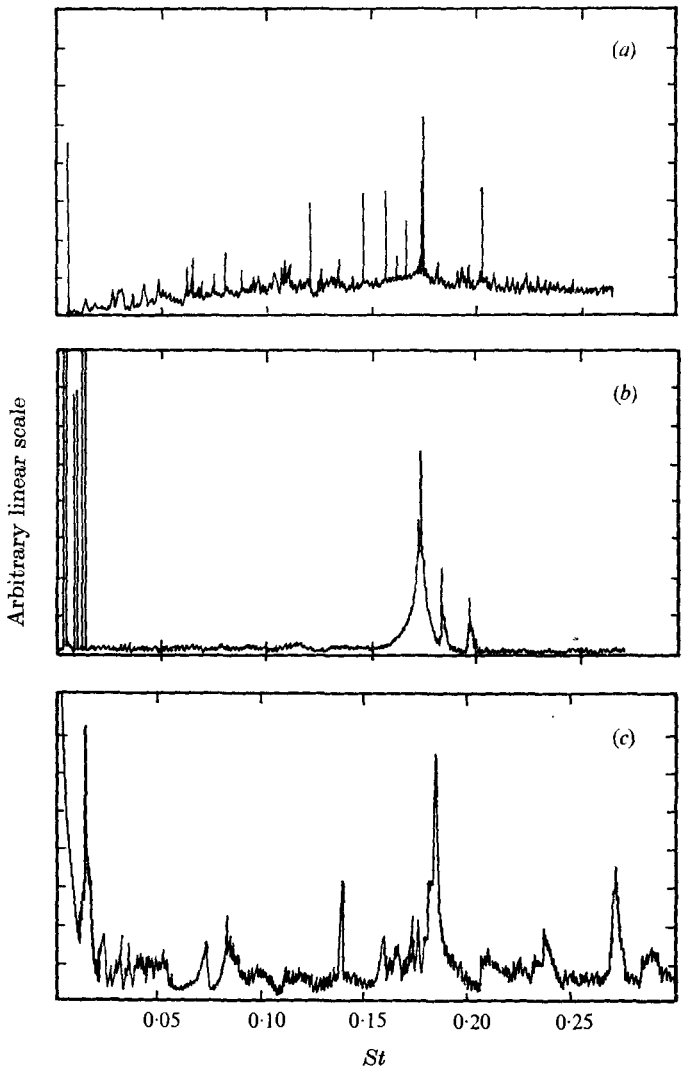

FIGURE 5. Microphone spectra in the near radiation field of the supersonic jet. Passband is 6 Hz; sweep rate is 1000 Hz min^{-1}.

	D (mm)	U/d	Re
(*a*)	6·35	105 000	14 400
(*b*)	9·52	67 800	11 000
(*c*)	15·9	38 700	8 060

as pump noise, etc.) were also measured; they were found to be 20 dB less than the lowest sound levels measured in the acoustic field.

Returning to figure 5, there are two comparisons which it is appropriate to make with these frequency spectra data. First, the largest frequency peak in all jets occurs at a non-dimensional frequency of approximately $St = 0{\cdot}18$, very close to the value predicted by Tam (1972) for the most dominant instability

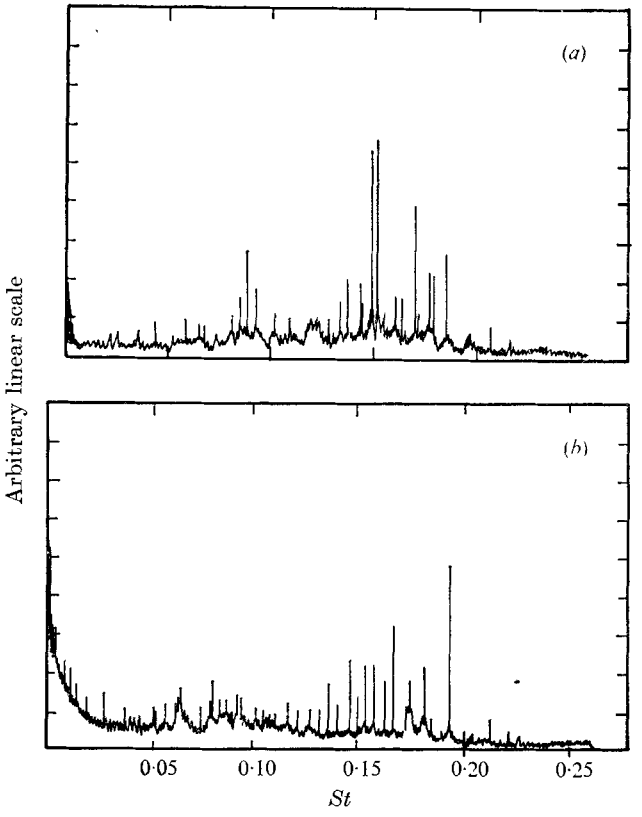

FIGURE 6. Spectra of hot-wire voltage fluctuations, recorded on different days. $D = 6{\cdot}35$ mm, $(x/D)_{\text{probe}} = 5$, $Re = 14\,600$.

mode. However, there is a discrepancy here, in that our measurements show in many cases three or more major spectral components, whereas Tam predicts a single frequency dominant mode. (He disregards a second predicted mode with a much shorter wavelength as being unimportant. This second mode is none of the major modes measured in the present study.) The multi-modal feature of the instability process was also observed by Westley (private communication) in the supersonic jet, and has been found in other supersonic flows such as wakes (McLaughlin 1971) and boundary layers (Kendall 1967). The second important comparison to make with the spectral data of figure 5 is with spectra measured by many investigators (e.g. Dosanjh & Yu 1968) of the noise radiation from high Reynolds number supersonic jets. The modes depicted in figure 5 are grouped around a Strouhal number of 0·18, which coincides with the maximum amplitude frequency of the rather broad spectra measured in high Reynolds number jets. Tam's thesis is that the major noise generation mechanism of the high Reynolds number jet is the large-scale instability, and the small-scale turbulence is responsible for broadening of the spectrum around the peak caused by the dominant oscillation. With this latest experimental evidence demonstrating several dominant modes, the hypothesis of the small-scale turbulence broadening the spectrum around the instability waves seems more plausible than ever.

A spectrum of the hot-wire voltage fluctuation measured in the flow field of the smallest jet is presented in figure 6 (*a*) for comparison with the microphone spectra of figure 5. For the measurements presented here, the hot wire was located 5 diameters downstream of the jet exit at the radial location of maximum fluctuations. The data at 5 diameters is presented, since it is far enough downstream for sufficient instability development, and is upstream of the nonlinear saturation, which is accompanied by frequency broadening. It is important to note that the frequency peaks do not shift as the probe is traversed axially.

A number of the peak amplitude frequencies in the hot-wire spectra occur at the same Strouhal number as those in the microphone spectra. However, a number of differences between the hot-wire spectra and the previous microphone spectra may be noticed. Not all the modes present in this particular hot-wire spectrum are present in the microphone spectra, and the relative amplitudes of different modes appearing in both spectra are not consistent. The problem is put into clearer focus when we consider another hot-wire spectrum, shown in figure 6 (*b*), which has been recorded with almost identical mean flow conditions. What we are seeing is a tendency for the instability process to assume different modes of oscillation, depending on very small changes in the mean flow conditions. In particular, from numerous experiments using the three different diameter nozzles, different pressure balance conditions, and several different hot-wire and microphone probe geometries, we have concluded that the exact characteristics of the frequency spectra at a specified probe location depend upon four parameters. These parameters are the nozzle geometry, the pressure balance condition, the Reynolds number and the humidity of the supply air. (The mean jet Mach number varies as much as 10 % with extremes in the humidity of the room supply air.) From these experiments, conclusive evidence was obtained, showing the microphone frequency spectra to be almost indistinguishable from the hot-wire frequency spectra measured at the maximum fluctuation radius, provided all four parameters were identical.

The important conclusion to be drawn from this series of measurements is that the multi-modal phenomenon is not a peculiarity of our facility, but characteristic of supersonic jets in this low Reynolds number range.

Re-examining figure 5 (*b*) it may be noticed that the spectrum measured with the intermediate size jet tends to have one large dominant spectral component. In fact, numerous hot-wire measurements presented in McLaughlin & McColgan (1974) showed, in most cases, only a single instability mode. The single instability mode behaviour is predicted by Tam (1972), who demonstrated that the frequency selection process is controlled by the wave-cell structure. This leads us to re-examine the relative strengths of the wave cells of the two smaller nozzles as depicted in figure 3. Here we found that the wave-cell structure is stronger in the 9·52 mm jet compared with the 6·35 mm jet. This is consistent with the tendency for the 9·52 mm jet to have a stronger frequency selectivity of a single mode. We assume that the wave-cell structure of the 15·9 mm jet is also weaker than the intermediate size jet, since that nozzle is contoured to provide parallel flow at the exit. Again the tendency for multi-modes is more prevalent in the jet with presumably weaker cell structure.

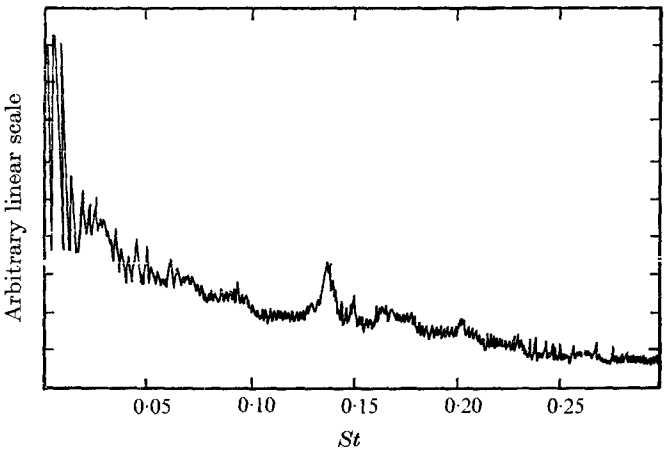

FIGURE 7. Spectrum of hot-wire voltage fluctuations. $D = 9{\cdot}52$ mm, $(x/D)_{\text{probe}} = 5$, $Re = 107\,000$.

It appears that, for well-constructed parallel flow nozzles, the mode selection process in Tam's (1972) analysis is inadequate to predict the actual phenomena in the design pressure ratio condition. We suggest that this is one part of the analysis which should be modified. Hopefully that can be done without completely eliminating the mode selection process from the analysis, since the theory predicts a Strouhal number in the range of the dominant modes in the jets.

All the spectra presented heretofore were for jets in the Reynolds number range 8060–14 500. As the Reynolds number is increased, the spectra broaden to become more similar to the spectra of Dosanjh & Yu (1968). In fact, the hot-wire spectrum in figure 7 is at a Reynolds number of 107 000, which is intermediate between the present low Reynolds number data and the higher Reynolds number data of Dosanjh & Yu. There is a much greater breadth to the spectrum, but there is still a distinct peak close to the same Strouhal number as the low *Re* experiments. This is a strong indication that the instability waves are still a major portion of the turbulence in the jet.

3.3. *Microphone amplitude measurements*

Microphone measurements were made in the acoustic field of the perfectly expanded 6·35 mm jet at a Reynolds number of 12 600. Figure 8 presents sound pressure level contours determined from this data. The general shape of the contours is in good agreement with the measurements of Mayes, Lanford & Hubbard (1959), Yu & Dosanjh (1972) and Louis, Letty & Patel (1972) in high Reynolds number jets in the Mach number range 1·5–2·75.

In addition to the shape of the contours a comparison can be made of the magnitudes of the sound pressure levels in the low and high Reynolds number jets (at the same non-dimensional locations). To make a meaningful comparison 34 dB must be added to the present measurements to scale the ambient pressure ($p_{\text{ch}} = 0{\cdot}02$ atm) up to the exhaust pressure of the atmosphere used in the high Reynolds number tests. The values of the sound pressure levels adjusted in this

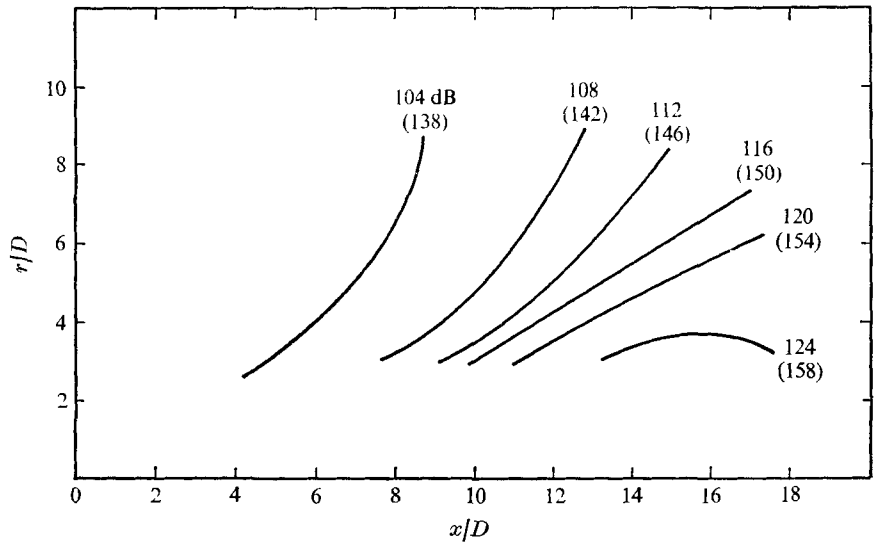

FIGURE 8. Microphone constant-amplitude noise-contours. Amplitudes scaled at atmospheric exhaust pressure in parentheses. $D = 6{\cdot}35$ mm, $p_n/p_{ch} = 1{\cdot}01$, $Re = 12\,600$.

manner are given in parentheses in figure 8. These values approach the levels measured in the high Reynolds number jets at similar non-dimensional locations. No direct comparisons can be made because of the differences in the flow conditions (particularly Mach number). But a general comparison shows enough similarity between the low and high Reynolds number measurements to indicate that the major noise producing mechanisms are similar.

3.4. *Hot-wire fluctuation amplitude measurements*

Figure 9 presents comparative evidence on the profiles of hot-wire fluctuations at various locations downstream from the jet exit. These measurements were made at a low Reynolds number ($Re = 14\,700$) and a Reynolds number about three times as large. The general shapes of the fluctuation distributions are similar, except that the higher Reynolds number jet has a peak fluctuation amplitude of over 5 % within a diameter of the exit. Figure 10 is a plot of the peak r.m.s. hot-wire voltage fluctuations against the downstream co-ordinate. Note that the low Reynolds number growth is approximately exponential (up to the nonlinear region), whereas the high Reynolds number case has initial fluctuations almost as high as the downstream level. There is, however, a considerable amount of low-frequency content in the higher Reynolds number jet, particularly near the jet exit. Since the low-frequency components are enhanced by the resonance of the finite-size test chamber, they do not give a fair representation of the fluctuations one obtains in the free-field jet. For this reason, a second set of peak amplitude distributions is presented in figure 11, which have the spectral components below 1000 Hz, as well as those above 50 000 Hz, removed. These distributions are probably more representative of the free-field jet fluctuations. They indicate that the supersonic jet in the Reynolds number range 14 000–44 100 is

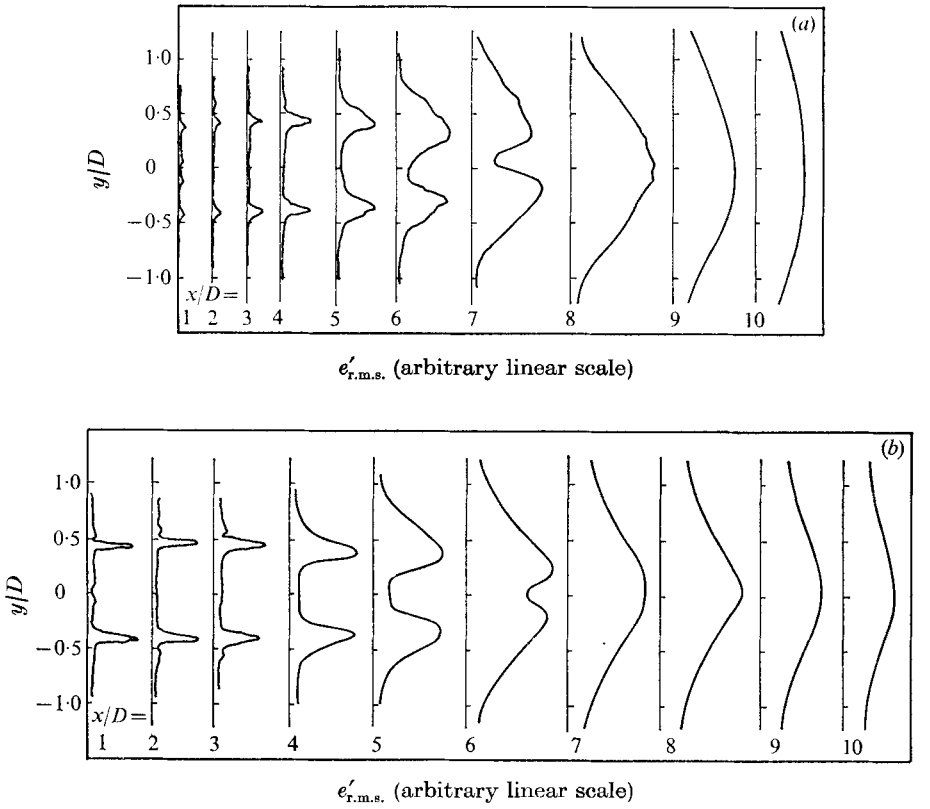

FIGURE 9. Profiles of r.m.s. hot-wire voltage fluctuations at various downstream locations in the jet. D = 9·52 mm. Re: (*a*) 14 700, (*b*) 44 100.

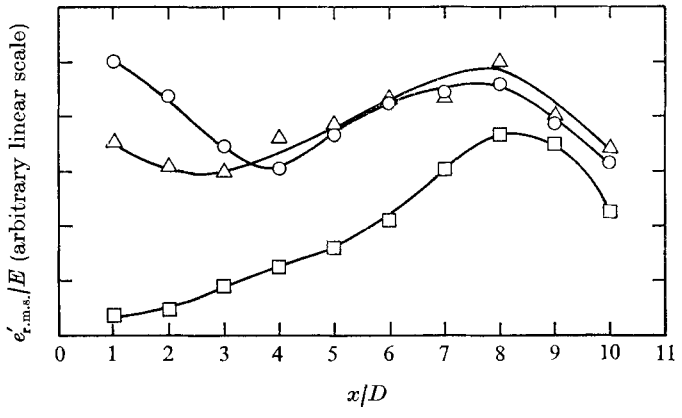

FIGURE 10. Axial distribution of peak hot-wire voltage fluctuations. Passband is 0·2–50 kHz.

	□	○	△
Re	14 700	29 300	44 000

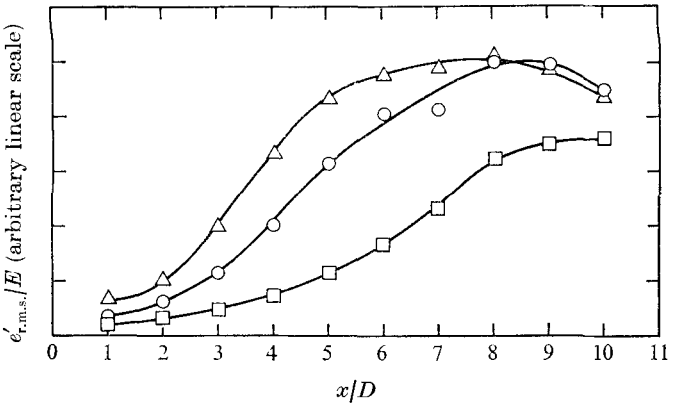

FIGURE 11. Axial distribution of peak hot-wire voltage fluctuations. Passband is 1–50 kHz.

	□	○	△
Re	14900	30000	45400

undergoing a transition process, in which the initial oscillations are growing almost exponentially. This suggests that an instability theory is appropriate to apply directly to the supersonic jet in this low Reynolds number regime.

3.5. *Instability excitation and phase measurements*

As discussed earlier, the phase measurements were made by artificially exciting one of the dominant modes of the instability and measuring the distribution of phases either within the jet with the hot wire, or in the radiation field, with the microphone. In either case, the phase difference between the excitation signal and the spectral component of the sensor signal provided the distribution of relative phases in the region of measurement.

Before presenting the results of the phase measurements, it is important to evaluate the effect of the excitation on the naturally occurring instability development. In the case of the 9·52 mm jet, in which only one spectral component dominates, excitation at the natural frequency effected no perceptible change in the spectrum in figure 5 (*b*). For these measurements, the amplitude of the hot-wire voltage fluctuations remained almost the same. The only apparent change indicated by the oscilloscope was that the hot-wire signal phase locked to the excitation signal. During the experiment, the amplitude of the glow discharge exciter was increased to a level at which the instability waves phase lock onto the excitation signal with some degree of reliability.

Artificial excitation of the 6·35 mm jet was by no means as straightforward, as in the 9·52 mm jet. Since the frequency spectra contained several dominant modes, it was necessary to choose which mode to excite (or do several sets of measurements). For reasons not well understood, certain major modes phase lock to the excitation much more dependably than others. This was the major determining factor in choosing excitation frequencies of $f = 19400$ and 22300 Hz ($St = 0{\cdot}18$ and $0{\cdot}21$, respectively). Moreover, the Strouhal number of $St = 0{\cdot}18$ was close to the value of $St = 0{\cdot}17$ of the mode excited in the 9·52 mm jet.

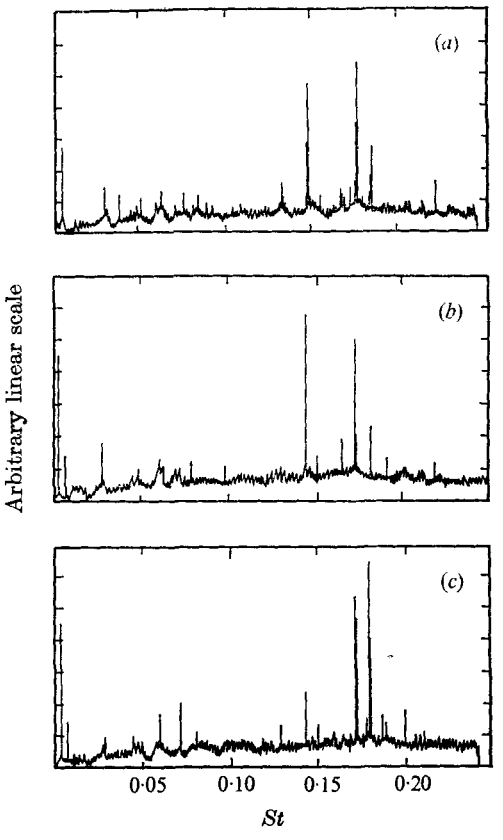

FIGURE 13. Effect of excitation on the microphone spectrum of the 6·35 mm jet. Re = 14 400. (*a*) Naturally excited. (*b*) St_{exciter} = 0·14. (*c*) St_{exciter} = 0·18.

Figure 12 (plate 1) demonstrates the extent of phase locking achieved. It is a typical oscilloscope photograph of a 0·1 ms time history of the excitation signal and the instantaneous hot-wire signal. In all phase measurements reported in this paper, the amplitude of the excitation was adjusted to give at least this degree of phase locking between the hot-wire or microphone signal and the excitation signal.

We recognize the limitations of this study; and we realize that it is important to determine the wave properties of all the dominant modes. However, some improvements in our excitation technique are needed before we shall be able to obtain reliable phase measurements with the other modes. Figure 13 demonstrates the effect of exciting the instability at different frequencies. Figure 13 (*a*) depicts a spectrum of the microphone signals in the acoustic field of the naturally excited jet, while figures 13 (*b*) and (*c*) depict the spectra of the microphone signal under identical conditions, except that the instability is artificially excited at 15 300 and 19 400 kHz (St = 0·14 and 0·18, respectively). The spectrum in figure 13 (*c*) is changed the most substantially, as the spectral component at the excitation frequency is greatly enhanced. This may partly demonstrate why that particular mode was most amenable to phase locking onto the excitation.

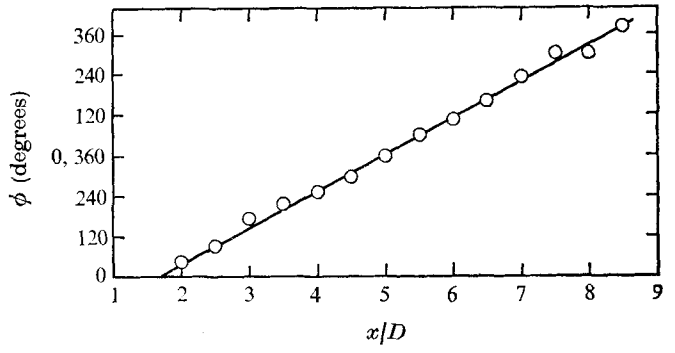

FIGURE 14. Axial distribution of hot-wire relative phase ϕ. D = 9·52 mm, Re = 14 700, St = 0·17.

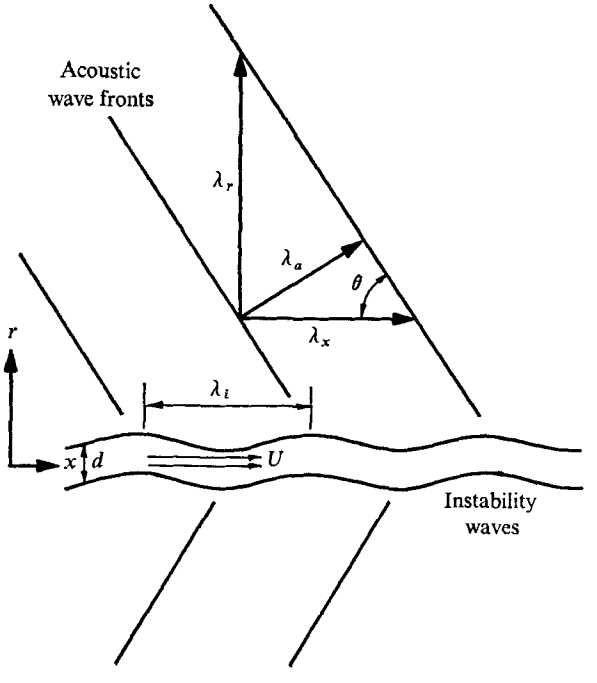

FIGURE 15. Orientation of acoustic and instability waves.

3.6. *Hot-wire phase measurements*

Numerous phase measurements were made from data such as those shown in figure 12 for a number of hot-wire probe locations. Figure 14 presents the results of phase measurements, in which the probe was located on the bottom shear layer at the point of maximum fluctuation for various downstream locations. The 9·52 mm jet was used in this test with M = 2·3 and Re = 14 700. A least squares linear regression analysis yielded a wavelength of $\lambda_i/D = 3{\cdot}36 \pm 0{\cdot}15$, where the uncertainty limits are the 95% confidence interval for the random error of the measurement. Figure 15 is a schematic of the waves.

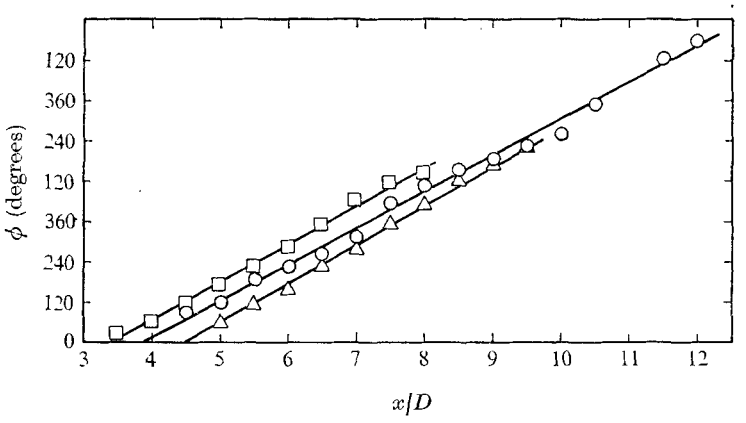

FIGURE 16. Axial distribution of hot-wire relative phase ϕ on different days.

	□	○	△
λ_i/D	$3{\cdot}18 \pm 0{\cdot}18$	$3{\cdot}34 \pm 0{\cdot}16$	$3{\cdot}03 \pm 0{\cdot}12$

Besides the random error, there was a small degree of systematic error from day to day due to changes in humidity, and/or the pressure balance condition. To help evaluate the systematic error, the instability wavelength λ_i was determined from measurements on three or more different days. Figure 16 shows the phase data taken on three different dates using the 6·35 mm jet. Notice that there is an apparent change in the location of the abscissa intercept. This effect can be interpreted as a change in the position of phase lock with the exciter. The exact reason for this shift is unknown at present.

It is encouraging that the important experimental measurements (namely, the slopes of the phase plot) are all in reasonable agreement. For the data plotted in figure 16, regression analysis yields the following wavelengths:

(i) $\lambda_i/D = 3{\cdot}18 \pm 0{\cdot}18$, (ii) $\lambda_i/D = 3{\cdot}34 \pm 0{\cdot}16$, (iii) $\lambda_i/D = 3{\cdot}03 \pm 0{\cdot}12$.

From these data we estimate the wavelength for this case to be $\lambda_i/D = 3{\cdot}20 \pm 0{\cdot}30$, the uncertainty limits including the random error indicated by the variance of the individual phase measurements, and the systematic error due to slight changes in experimental conditions. Similarly, the best estimate of the instability wavelength in the 9·52 mm jet was determined from data like those shown in figure 14 to be $\lambda_i/D = 3{\cdot}30 \pm 0{\cdot}30$.

Hot-wire phase measurements were also performed with the higher frequency ($St = 0{\cdot}21$) mode being excited (6·35 mm jet). The estimated instability wavelength for this mode was $\lambda_i/D = 2{\cdot}55 \pm 0{\cdot}25$, again based on a number of experiments on different days. Combining the wavelength and frequency, we calculated the wave speed to be $0{\cdot}67U$ (or $1{\cdot}18a_0$, where a_0 is the acoustic velocity of the surrounding air). The wave speed of the $St = 0{\cdot}18$ mode was $0{\cdot}73U$. Comparing the two modes, we conclude that the wave speeds agree within the accuracy of the measurement ($\pm 10\%$). To make any conclusive statement on the dispersive properties of the different frequency modes, more measurements are needed,

D (mm)	6·35		9·52	
M	2·2		2·3	
U/d (s^{-1})	105 000		67 800	
a_j/a_0	0·718		0·700	
	Measured	Predicted	Measured	Predicted
St	0·186	0·193	0·170	0·198
$k_i d$	1·61	1·47	1·60	1·50
λ_i/d	3·91	4·27	3·92	4·18
C/a_0	1·15	1·31	1·04	1·32
C/U	0·726	0·825	0·653	0·828

TABLE 1. Comparison of measured wave properties with predictions of Tam (1972). k_i is the wavenumber in the x direction, C is the wave speed, and a_j is the speed of sound in the jet.

particularly of modes with a greater frequency difference than those measured here.

We are also preparing to make phase measurements around the entire azimuth of the jet, to establish the azimuthal mode number n of the dominant mode (or modes in the case of the small jet). However, preliminary measurements have been made on both the top and bottom of the shear annulus, which indicate that the instability is out of phase by 180° across the jet. This strongly suggests that $n = 1$ is the azimuthal mode number of the dominant oscillation, and definitely rules out the $n = 0$ and 2 choices.

Assuming that the mode we are measuring is the $n = 1$ (or $n = -1$) mode, we have obtained the measurements to test Tam's theory (1972) for its ability to predict the frequency, wavelength and wave speed of the most dominant oscillation.

For this comparison, we use the data for the $St = 0{\cdot}18$ mode in the 6·35 mm jet, since this mode was the closest to the largest peak in noise spectra, as in figure 5 (*a*). The jet effective diameter d is used, rather than the nozzle exit diameter D for the data, which is listed in table 1.

The agreement between theory and experiment is close enough to conclude that Tam has developed a reliable analysis. This does not guarantee that his technique will be directly applicable to higher Reynolds number jets. But it certainly suggests that here is a strong foundation on which more complete, and no doubt much more complicated analyses may be formulated to handle the full scale jet noise problem.

3.7. *Acoustic phase measurements*

Relative phase measurements were made with the microphone in the acoustic field of both the 6·35 and 9·52 mm exit diameter jets. It is with these measurements that the greatest difficulty was encountered with change in the phase lock position noted earlier. In fact, the measurements with the larger nozzle were too unreliable to present here. Reliable measurements were obtained with the 6·35 mm jet when experimental conditions were closely monitored and constantly

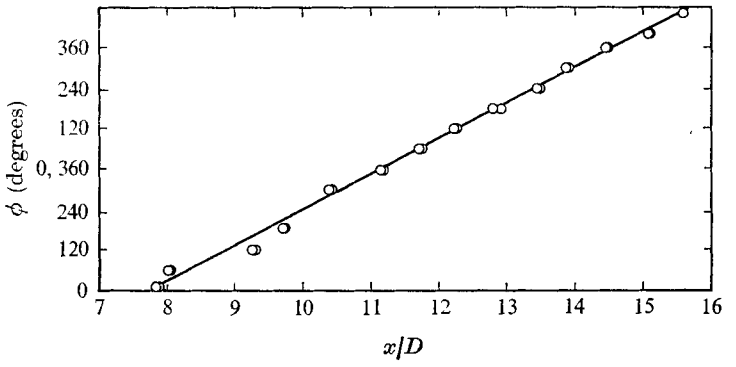

FIGURE 17. Axial distribution of microphone relative phase ϕ. $D = 6{\cdot}35$ mm, $Re = 11\,600$, $St = 0{\cdot}18$.

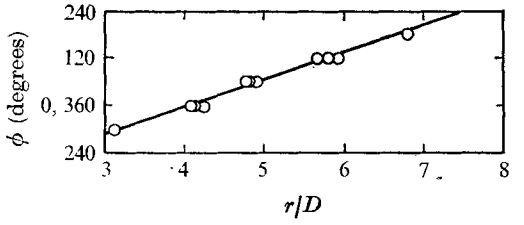

FIGURE 18. Radial distribution of microphone relative phase ϕ. $D = 6{\cdot}35$ mm, $Re = 11\,600$, $St = 0{\cdot}18$.

adjusted. In particular, the pressure balance condition was maintained between $1{\cdot}005 < p_n/p_{ch} < 1{\cdot}01$.

Figure 17 presents the results of relative phase measurements made at a radial location $r/D = 4$, in which the microphone probe was traversed in the x direction. The slope and its 95 % confidence interval determined from the least squares linear regression is $\lambda_x/D = 3{\cdot}35 \pm 0{\cdot}09$ for this data. Similarly, figure 18 presents the results of typical phase measurements made at $x/D = 11$, in which the probe was traversed in the radial (r) direction. Its slope is determined to be

$$\lambda_r/D = 5{\cdot}35 \pm 0{\cdot}45.$$

Experiments on several different days were performed in the manner outlined above; and a final average for all conditions is recorded in table 2. Data from the hot-wire phase measurements are included; also listed are the total estimated uncertainties, the number of days of experiments for each measurement, and the total number of individual phase measurements on all days. The wavelengths listed are our best estimates of the true values for the two jets. The Reynolds number range used in the experiments was 14 100–38 000; over this limited range no wavelength dependence on Reynolds number was apparent.

By using the wavelengths in the x and r directions, the wavelength perpendicular to the acoustic wave fronts in the zero azimuth plane, and the angle which the wave fronts make with the x axis can be determined. These are $\lambda_a/D = 2{\cdot}80 \pm 0{\cdot}25$ and $\theta = 57{\cdot}5° \pm 4°$, respectively (see figure 15). A calculation of the wave

		Best estimate	Total uncertainty	Number of experiments on different days	Total number of individual phase measurements
6·35 mm (M = 2·2) jet					
St = 0·18	λ_i/D	3·20	± 0·30 (10 %)	3	30
	λ_x/D	3·25	± 0·30 (10 %)	6	69
	λ_r/D	5·10	± 0·60 (12 %)	2	21
St = 0·21	λ_i/D	2·55	± 0·25 (10 %)	5	60
9·52 mm (M = 2·3) jet					
St = 0·17	λ_i/D	3·30	± 0·3 (10 %)	2	17

TABLE 2. Summary of wavelength measurements

speed from the frequency and wavelength gives a value of 332 m s^{-1}. This wave velocity agrees with the ambient speed of sound, a_0 = 342 m s^{-1}, within the accuracy of our measurements.

Another confirmation of our results is calculation of the Mach angle associated with the convection velocity of the instability waves in the jet (C = 392 m s^{-1}). This calculation yields $\mu = \sin^{-1} a_0/C = 60{\cdot}2 \pm 2°$, which is within the uncertainty of the measured acoustic wave angle. These measurements are in agreement with the concept that the noise radiated from the jet disturbances propagates like Mach waves. This agrees with some of the first work in supersonic jet noise analysis, by Ffowcs Williams (1963) and Phillips (1960).

Recent stability analyses have not dealt directly with the Mach wave issue for the dominant jet instability. Tam (1971) and Chan & Westley (1973) use a small wavelength approximation, in analysing the propagation direction of the noise radiated from the shear layers near the jet exit. Therefore, their theories do not apply to the noise radiated from the large-scale instabilities. It is not clear how the small wavelength approximation affects this prediction; therefore, we suggest that this part of the analysis should be re-examined. At the same time, more measurements of this phenomenon are needed, particularly over a range of jet Mach numbers.

4. Conclusions

Hot-wire measurements in the low Reynolds number supersonic jet demon strate that the initial disturbances, moving at a velocity greater than the ambient speed of sound, propagate and grow like instability waves. In fact, the measured wave properties of the St = 0·18 instability are in close agreement with the prediction of Tam (1972).

There are numerous major modes in the instability process of a perfectly-expanded supersonic jet, which contradicts the theory of Tam (1972). Comparison of the present frequency spectra with the results from high Reynolds number jets

suggests that the multi-modal instability phenomenon plays an important role in the development of the turbulence in the high Reynolds number jets. This we believe is an area of analysis where both experimental and theoretical efforts need to be extended.

Microphone measurements have shown that the wavelength, wave orientation and frequency of the acoustic radiation generated by the dominant instability agree with the Mach wave concept. The instability analyses, as presently formulated, need to be re-examined with respect to this issue to ensure that there are no inconsistencies between theory and experiment.

The sound pressure levels measured in the low Reynolds number jet extrapolate to values approaching the noise levels measured by other experimenters with high Reynolds number jets. These measurements provide more evidence to suggest that the dominant noise generation mechanism in high Reynolds number jets is the large-scale instability.

This research was supported by the National Science Foundation under grant GK-32686. The authors would like to acknowledge the helpful suggestions of Professor C. K. W. Tam, of Florida State University, and Professor W. G. Tiederman, of Oklahoma State University.

REFERENCES

BEHRENS, W. 1963 Viscous interaction effect on a static pressure probe at $M = 6$. *A.I.A.A. J.* **1**, 2364–2366.

BEHRENS, W. 1968 Far wake behind cylinders at hypersonic speeds. II. Stability. *A.I.A.A. J.* **6**, 225–232.

BISHOP, K. A., FFOWCS WILLIAMS, J. E. & SMITH, W. 1971 On the noise sources of the unsuppressed high-speed jet. *J. Fluid Mech.* **50**, 21–31.

CHAN, Y. Y. & WESTLEY, R. 1973 Directional acoustic radiation generated by spatial jet instability. *CASI Trans.* **6**, 36–41.

CROW, S. C. & CHAMPAGNE, F. H. 1971 Orderly structure in jet turbulence. *J. Fluid Mech.* **48**, 547–591.

DEWEY, C. F. 1965 A correlation of convective heat transfer and recovery temperature data for cylinders in compressible flow. *Int. J. Heat Mass Transfer*, **8**, 245–252.

DOSANJH, D. S. & YU, J. C. 1968 Noise from underexpanded axisymmetric jet flow using radial jet impingement. *Proc. AFOSR-UTIAS Symp. on Aerodynamic Noise.* Toronto, Canada.

FFOWCS WILLIAMS, J. E. 1963 The noise from turbulence convected at high speed. *Phil. Trans.* A **255**, 459.

KENDALL, J. M. 1967 Supersonic boundary layer stability experiments. *Proc. Boundary Layer Trans. Study Group, Meeting*, II, *Aerospace Rep.* TR-0158 (S3816-63)-1.

LEE, H. K. & RIBNER, H. S. 1972 Direct correlation of noise and flow of a jet. *J. Acoust. Soc. Am.* **52**, 1280–1290.

LIGHTHILL, M. J. 1952 On sound generated aerodynamically. I. General theory. *Proc. Roy. Soc.* A **211**, 564–587.

LIGHTHILL, M. J. 1954 On sound generated aerodynamically. II. Turbulence as a source of sound. *Proc. Roy. Soc.* A **222**, 1–32.

LILLEY, G. M., MORRIS, P. & TESTER, B. J. 1973 On the theory of jet noise and its applications. *A.I.A.A. Paper*, no. 73-987.

LOUIS, J. F., LETTY, R. P. & PATEL, J. R. 1972 A systematic study of supersonic jet noise. *A.I.A.A. Paper*, no. 72-641.

MCLAUGHLIN, D. K. 1971 Experimental investigation of the stability of the laminar supersonic cone wake. *A.I.A.A. J.* **9**, 696–702.

MCLAUGHLIN, D. K. & MCCOLGAN, C. J. 1974 Hot-wire measurements in a supersonic jet at low Reynolds numbers. *A.I.A.A. J.* **12**, 1279–1281.

MATTHEWS, M. L. 1958 An experimental investigation of viscous effects on static and impact pressure probes in hypersonic flow. *GALCIT, Hypersonic Research Project, Memo.* no. 44. Pasadena, California.

MAYES, W. H., LANFORD, W. D. & HUBBARD, H. H. 1959 Near field and far field noise surveys of solid fuel rocket engines for a range of nozzle exit pressures. *N.A.S.A. Tech. Note*, no. D-21.

MORKOVIN, M. W. 1956 Fluctuations and hot-wire anemometry in compressible flows. *AGARDograph*, no. 24.

PHILLIPS, O. M. 1960 On the generation of sound by supersonic turbulent shear layers. *J. Fluid Mech.* **9**, 1–28.

RIBNER, H. S. 1969 Eddy–Mach wave noise from a simplified model of a supersonic mixing layer. *Basic Aerodynamic Noise Research, N.A.S.A.* SP-207.

SEDEL'NIKOV, T. K. 1967 The frequency spectrum of the noise of a supersonic jet. *Phy. Aero. Noise*. Moscow: Nauka. (Trans. 1969 *N.A.S.A.* TTF-538, 71–75.)

TAM, C. K. W. 1971 Directional acoustic radiation from a supersonic jet generated by shear layer instability. *J. Fluid Mech.* **46**, 757–768.

TAM, C. K. W. 1972 On the noise of a nearly ideally expanded supersonic jet. *J. Fluid Mech.* **51**, 69–95.

TAM, C. K. W. 1973 Supersonic jet noise generated by large scale disturbances. *A.I.A.A. Paper*, no. 73-992.

YU, J. C. & DOSANJH, D. S. 1972 Noise field of a supersonic Mach 1·5 cold model jet. *J. Acoust. Soc. Am.* **51**, 1400.

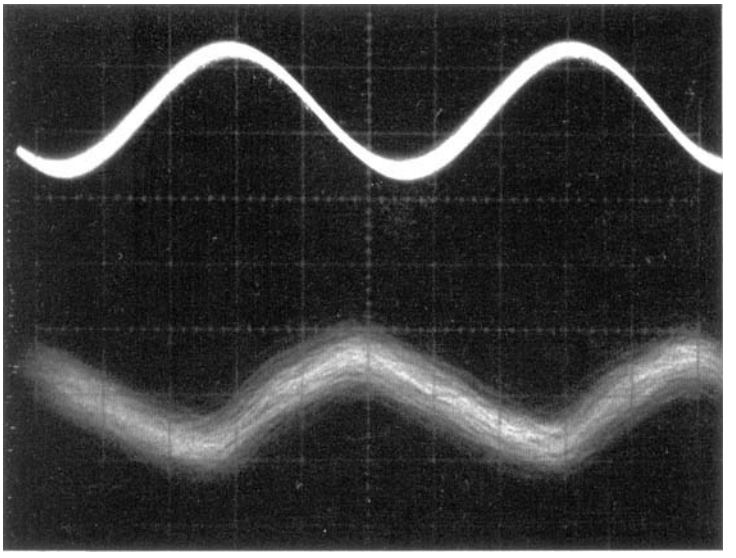

FIGURE 12. Oscilloscope trace of exciter signal (upper trace), and instantaneous hot-wire signal (lower), showing a typical phase-locked situation. $D = 6{\cdot}35$ mm, $Re = 19\,100$, $St_{\text{exciter}} = 0{\cdot}18$, $(x/D)_{\text{probe}} = 5$, sweep rate $= 10\ \mu\text{s cm}^{-1}$.